International Journal of Heat and Mass Transfer 159 (2020) 120133

Contents lists available at ScienceDirect

International Journal of Heat and Mass Transfer

journal homepage: www.elsevier.com/locate/hmt

Controlling thermal waves with transformation complex thermotics

Liujun Xu*, Jiping Huang*

Department of Physics, State Key Laboratory of Surface Physics, and Key Laboratory of Micro and Nano Photonic Structures (MOE), Fudan University, Shanghai 200438, China

ARTICLE INFO

Article history:
Received 3 May 2020
Revised 16 June 2020
Accepted 26 June 2020

Keywords:
Complex thermal conductivity
Complex conduction equation
Transformation complex thermotics
Thermal conduction-convection

ABSTRACT

Conduction and convection are two fundamental methods of heat transfer, which are generally considered independent. We manage to unify them by coining a complex thermal conductivity whose real and imaginary parts are related to conduction and convection, respectively. Accordingly, the conduction-convection process with thermal waves is dominated by the complex conduction equation, thus called complex thermotics herein. To go further, we establish the theory of transformation complex thermotics by proving the form-invariance of the complex conduction equation and deriving the transformation principle of complex thermal conductivities. As model applications, we design three devices with functions of cloaking, concentrating, and rotating thermal waves. Moreover, experimental demonstration is suggested with a porous medium whose effective complex thermal conductivity is calculated with the method of weighted average. These findings could broaden the fundamental knowledge of conduction and convection, and have potential applications in designing thermal metamaterials.

© 2020 Elsevier Ltd. All rights reserved.

1. Introduction

Conduction and convection are ubiquitous in nature, whose key parameters are mainly thermal conductivity and convective velocity, respectively. Therefore, these two methods are generally considered independent, which makes their simultaneous manipulation challenging. Recently, transformation theories have been proposed to control conduction and convection simultaneously, yielding practical applications such as cloaking, concentrating, and rotating [1–3]. These theories are applicable for constant-temperature boundary conditions, but not necessarily appropriate for periodic boundary conditions with thermal waves.

To solve the problem, we resort to a complex thermal conductivity $\kappa = \sigma + \mathrm{i}\tau$ with σ and τ being two real numbers [4]. The κ can be well understood with the complex plane shown in Fig. 1. We consider thermal waves and suppose convective velocities to be rightward. The thermal waves in the right ($\sigma > 0$) and left ($\sigma < 0$) half planes have loss and gain of amplitude, respectively. The motion of the thermal waves in the upper ($\tau > 0$) and lower ($\tau < 0$) half planes is rightward and leftward, respectively. The conduction-convection process with thermal waves is dominated by the complex conduction equation, thus called complex thermotics herein. In other words, convection can be regarded as a complex form of conduction.

Accordingly, we study the complex conduction equation and propose the theory of transformation complex thermotics, which bridges spatial transformations and material transformations. We prove the form-invariance of the complex conduction equation under coordinate transformations and derive the transformation rule of complex thermal conductivities. Transformation complex thermotics also allows us to design cloaking, concentrating, and rotating as three model applications. Concretely speaking, cloaking can hide an obstacle without distorting the thermal wave in the background; concentrating can enhance the density of thermal wave (indicating a larger heat flux); and rotating can control the direction of thermal wave. We further provide experimental suggestions with a porous medium whose effective complex thermal conductivity is calculated with the method of weighted average. The application range of transformation complex thermotics is also extended from pure materials to composite materials. Let us start from establishing the transformation theory.

2. Theory of transformation complex thermotics

Complex thermotics is dominated by the complex conduction equation,

$$\rho C \partial T/\partial t + \boldsymbol{\nabla} \cdot (-\kappa \boldsymbol{\nabla} T) = 0, \tag{1}$$

where ρ, C, κ, T, and t are density, heat capacity, complex thermal conductivity, temperature, and time, respectively. Here the complex thermal conductivity κ can be expressed as [4]

$$\kappa = \sigma + \mathrm{i}\tau = \sigma + \mathrm{i}\frac{\rho C \boldsymbol{v} \cdot \boldsymbol{\beta}}{\beta^2}, \tag{2}$$

where $\boldsymbol{v}$ is convective velocity, and $\boldsymbol{\beta}$ is wave vector. By applying a wave-like temperature profile [5,6] denoted as $T = A_0 \mathrm{e}^{\mathrm{i}(\boldsymbol{\beta}\cdot\boldsymbol{r}-\omega t)} + T_0$, the dispersion relation of complex thermotics can be derived,

$$\omega = \boldsymbol{v} \cdot \boldsymbol{\beta} - \mathrm{i}\frac{\sigma \beta^2}{\rho C}, \tag{3}$$

where A_0, $\boldsymbol{r}$, ω, and T_0 are the amplitude, position vector, frequency, and reference temperature of the wave-like temperature profile, respectively. Such a wave-like temperature profile can also be called a thermal wave because it is

* Corresponding authors.
E-mail addresses: 13307110076@fudan.edu.cn (L. Xu), jphuang@fudan.edu.cn (J. Huang).

https://doi.org/10.1016/j.ijheatmasstransfer.2020.120133
0017-9310/© 2020 Elsevier Ltd. All rights reserved.

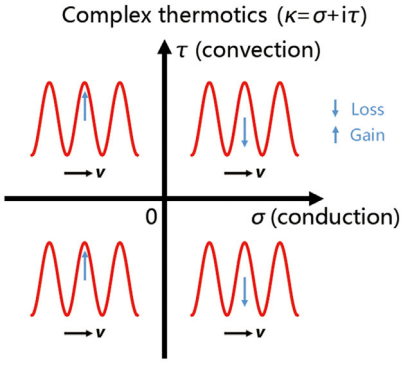

Fig. 1. Connotation of complex thermal conductivity $\kappa = \sigma + \mathrm{i}\tau$. Solid curves denote thermal waves. Convective velocities are supposed to be rightward. The arrow in the center of each thermal wave indicates loss or gain.

just a plane wave. Certainly, thermal waves in this work have a distinct mechanism from the Maxwell-Cattaneo heat waves [7,8]. Eq. (2) is a mathematical skill to unify conduction and convection. Due to the feature of thermal waves (say, $\nabla T = \mathrm{i}\boldsymbol{\beta} T$), we can derive $\mathrm{i}\tau \cdot \nabla T = -\tau\boldsymbol{\beta} T$ which just corresponds to a convective term.

Then, we prove that the complex conduction equation [Eq. (1)] is form-invariant under the spatial transformation from a curvilinear space X to a physical space X'. For this purpose, we rewrite Eq. (1) as

$$\rho C \partial T/\partial t + \nabla \cdot (-\sigma \nabla T) + \nabla \cdot (\tau \boldsymbol{\beta} T) = 0. \tag{4}$$

We suppose $\boldsymbol{u} = \tau\boldsymbol{\beta}$ and write down the component form of Eq. (4) in the curvilinear space with a contravariant basis $(\boldsymbol{g}^j, \boldsymbol{g}^k, \boldsymbol{g}^l)$ and contravariant components (x^j, x^k, x^l),

$$\sqrt{g}\rho C \partial_t T + \partial_j\left(-\sqrt{g}\sigma^{jk}\partial_k T\right) + \partial_j\left(\sqrt{g}u^j T\right) = 0, \tag{5}$$

where g is the determinant of the matrix $\boldsymbol{g}_p \cdot \boldsymbol{g}_q$ [p and q take on j, k or l with $(\boldsymbol{g}_j, \boldsymbol{g}_k, \boldsymbol{g}_l)$ being a covariant basis]. Eq. (5) is expressed in the curvilinear space, and then we rewrite it in the physical space with Cartesian coordinates $\left(x^{j'}, x^{k'}, x^{l'}\right)$,

$$\sqrt{g}\rho C \partial_t T + \partial_{j'}\frac{\partial x^{j'}}{\partial x^j}\left(-\sqrt{g}\sigma^{jk}\frac{\partial x^{k'}}{\partial x^k}\partial_{k'} T\right) + \partial_{j'}\frac{\partial x^{j'}}{\partial x^j}\left(\sqrt{g}u^j T\right) = 0, \tag{6}$$

where $\partial x^{j'}/\partial x^j$ and $\partial x^{k'}/\partial x^k$ are the components of the Jacobian transformation matrix $\tilde{J}$, and $\sqrt{g} = 1/\det \tilde{J}$. We turn the spatial transformation into the transformation of materials or vectors, so Eq. (6) becomes

$$\frac{\rho C}{\det \tilde{J}}\partial_t T + \partial_{j'}\left(-\frac{\frac{\partial x^{j'}}{\partial x^j}\sigma^{jk}\frac{\partial x^{k'}}{\partial x^k}}{\det \tilde{J}}\partial_{k'} T\right) + \partial_{j'}\left(\frac{\frac{\partial x^{j'}}{\partial x^j}u^j}{\det \tilde{J}} T\right) = 0. \tag{7}$$

The transformation rule can be derived,

$$(\rho C)' = \frac{\rho C}{\det \tilde{J}}, \tag{8a}$$

$$\sigma' = \frac{\tilde{J}\sigma\tilde{J}^S}{\det \tilde{J}}, \tag{8b}$$

$$\boldsymbol{u}' = \frac{\tilde{J}\boldsymbol{u}}{\det \tilde{J}}, \tag{8c}$$

where $\tilde{J}^S$ represents the transpose of $\tilde{J}$. Since $\boldsymbol{u} = \tau\boldsymbol{\beta}$, Eq. (8c) becomes

$$(\tau\boldsymbol{\beta})' = \frac{\tilde{J}(\tau\boldsymbol{\beta})}{\det \tilde{J}}. \tag{9}$$

We do not transform the wave vector, yielding $\boldsymbol{\beta}' = \boldsymbol{\beta}$, so Eq. (9) turns into

$$\tau' = \frac{\tilde{J}\tau}{\det \tilde{J}}. \tag{10}$$

Therefore, the transformation rule of complex thermotics can be summarized as

$$(\rho C)' = \frac{\rho C}{\det \tilde{J}}, \tag{11a}$$

$$\sigma' = \frac{\tilde{J}\sigma\tilde{J}^S}{\det \tilde{J}}, \tag{11b}$$

$$\tau' = \frac{\tilde{J}\tau}{\det \tilde{J}}. \tag{11c}$$

Eq. (11) is the first key result of this work, which gives the transformation principle of complex thermal conductivities. Physically speaking, Eqs. (11a) and (11b) agree with the result given by transformation thermotics for conduction [9,10]. Here a crucial point is to show that Eq. (11c) does not violate physical laws either. For this purpose, we substitute the concrete expression of τ [Eq. (2)] into Eq. (11c), thus yielding

$$\left(\frac{\rho C\boldsymbol{v}\cdot\boldsymbol{\beta}}{\beta^2}\right)' = \frac{\tilde{J}\left(\frac{\rho C\boldsymbol{v}\cdot\boldsymbol{\beta}}{\beta^2}\right)}{\det \tilde{J}}. \tag{12}$$

With Eq. (11a) and $\boldsymbol{\beta}' = \boldsymbol{\beta}$, Eq. (12) can be reduced to

$$\boldsymbol{v}' = \tilde{J}\boldsymbol{v}, \tag{13}$$

which also agrees with transformation thermotics for convection [1–3]. So far, we may briefly summarize two conclusions: (I) complex thermotics indicates that the real and imaginary parts of a complex thermal conductivity [Eq. (2)] are related to conduction (featured by dissipation) and convection (featured by propagation), respectively; and (II) the dominant equation of complex thermotics [Eq. (1)] is form-invariant under coordinate transformations.

3. Applications of transformation complex thermotics

The form-invariance of the complex conduction equation [Eq. (1)] allows us to design cloaking, concentrating, and rotating. A schematic diagram of cloaking is shown in Fig. 2(a). The left and right ends are set with a periodic boundary condition, say, $T_L = T_R$. The upper and lower boundaries are insulated. We consider the case with $\boldsymbol{v}//\boldsymbol{\beta}$ where the imaginary part of κ appears, as predicted by Eq. (2). We take on the wave vector $\beta = 2\pi m/W$ with $m = 10$, and the period of the thermal wave is $t_0 = 20$ s according to Eq. (3). We set the initial wave-like temperature profile as $T = 40\sin(\beta x) + 323$ K [see Fig. 2(b)]. When there is an obstacle without motion in the center, the thermal wave is distorted [see Figs. 2(c) and 2(d)]. Different from the methods with analytical design [11–13] or topology optimization [14–17] to design thermal cloaking, here we apply the present theory of transformation complex thermotics which follows $r = ar' + b$ and $\theta = \theta'$, where (r, θ) denote cylindrical coordinates in the physical space, $a = (r_2 - r_1)/r_2$, and $b = r_1$. Here r_1 and r_2 are the inner and outer radii of the shell, respectively. The Jacobian transformation matrix $\tilde{J}$ can be calculated as $\tilde{J} = \mathrm{diag}[a, ar/(r-b)]$. We design the cloak according to Eq. (11). The initial wave-like temperature profile in the cloak also turns into $T = 40\sin\{\beta[(r-b)x/(ar)]\} + 323$ K [see Fig. 2(e)]. Here the wave vector β is not transformed indeed, and only the coordinate x becomes $(r-b)x/(ar)$. Clearly, the obstacle does not distort the thermal wave in the background, and the cloaking effect is achieved [see Fig. 2(f) and (g)]. Since the dispersion relation [Eq. (3)] indicates that the decay rate [-Im(ω)] is in direct proportion to thermal conductivity, the temperature of the obstacle (with high thermal conductivity of 120 W m^{-1} K^{-1}) decays quickly and becomes a constant. Meanwhile, the thermal wave has amplitude loss due to the positive real part of κ, and propagates rightwards along x axis due to the positive imaginary part of κ. After propagating for a period (20 s), the thermal wave approximately gains a phase difference of 2π, thus going back to the initial position [see Fig. 2(e) and (g)].

With the similar method of cloaking, we can also design concentrating and rotating. The transformation of concentrating is $r = cr'$ for $0 < r' < r_m$, $r = dr' + f$ for $r_m < r' < r_2$, and $\theta = \theta'$. Here $c = r_1/r_m$, $d = (r_2 - r_1)/(r_2 - r_m)$, $f = (r_1 - r_m)r_2/(r_2 - r_m)$, and r_m is an intermediate radius between r_1 and r_2. The concentrating effect is determined by the parameter $1/c = r_m/r_1$, whose maximum value is r_2/r_1. Therefore, increasing the value of r_m can enhance the thermal gradient inside the concentrator. We can derive the Jacobian matrix $\tilde{J}$ in the core as $\tilde{J} = \mathrm{diag}[c, c]$, and that for the shell as $\tilde{J} = \mathrm{diag}[d, dr/(r-f)]$. The initial wave-like temperature profile in the core turns into $T = 40\sin[\beta(x/c)] + 323$ K, and that in the shell becomes $T = 40\sin\{\beta[(r-f)x/(dr)]\} + 323$ K [see

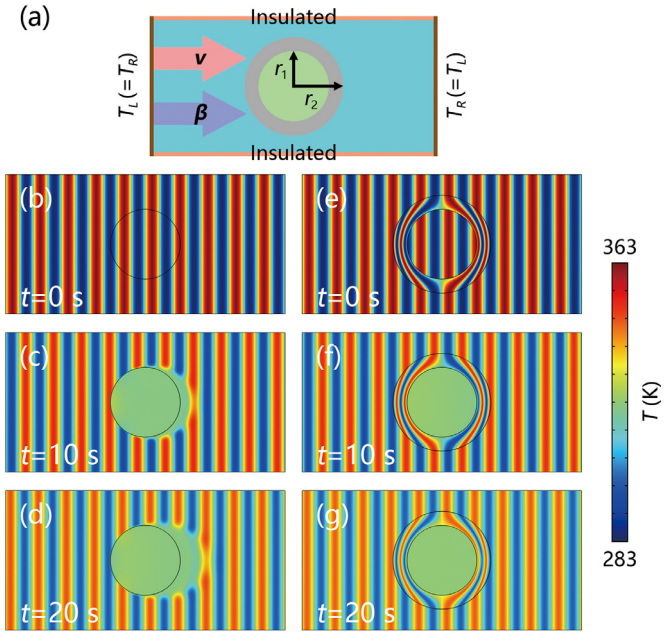

Fig. 2. (a) Schematic diagram of cloaking. (b)-(d) Simulations with an obstacle in the center. (e)-(g) Simulations with an obstacle coated by a cloak. Background parameters: $W = 20$ cm, $H = 10$ cm, $\rho = 1000$ kg/m^3, $C = 4200$ J kg^{-1} K^{-1}, $\sigma = 0.6$ W m^{-1} K^{-1}, and $v = 0.1$ cm/s. The obstacle is without motion, and has only a different parameter of $\sigma = 120$ W m^{-1} K^{-1} from background parameters. Cloaking parameters: the product of density and heat capacity is $\rho C(r-b)/\left(a^2 r\right)$; the real part of the complex thermal conductivity is diag$[(r-b)\sigma/r,\ r\sigma/(r-b)]$; and the velocity is $v[a\cos\theta,\ -ar\sin\theta/(r-b)]^c$ with $r_1 = 2.5$ cm, $r_2 = 3.5$ cm, $a = 2/7$ and $b = 2.5$ cm.

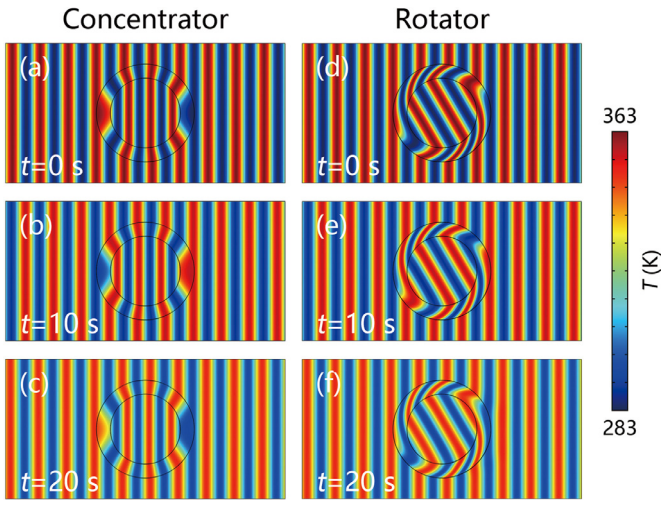

Fig. 3. Simulations of (a)-(c) concentrating and (d)-(f) rotating. The system sizes (W, H, r_1, and r_2) and background parameters (ρ, C, σ, and v) are the same as those for Fig. 2. Core parameters in (a)-(c): $\rho C/c^2$, σ, and cv. Shell parameters in (a)-(c): $\rho C(r-f)/\left(d^2 r\right)$, diag$[(r-f)\sigma/r,\ r\sigma/(r-f)]$, and $v[d\cos\theta,\ -dr\sin\theta/(r-f)]^c$ with $r_m = 3.2$ cm, $c = 25/32$, $d = 10/3$, and $f = -49/6$ cm. Core parameters in (d)-(f): ρC, σ, and $v[\cos\theta_0, \sin\theta_0]^c$. Shell parameters in (d)-(f): ρC, $\sigma\left[(1,\ hr),\ \left(hr,\ h^2r^2+1\right)\right]$, and $v[\cos\theta,\ hr\cos\theta - \sin\theta]^c$ with $\theta_0 = \pi/6$ rad and $h = -\pi/6$ rad/cm.

Fig. 3(a)]. The thermal waves at $t = 10$ s and $t = 20$ s are shown in Fig. 3(b) and (c), respectively. Clearly, the thermal wave in the center is concentrated.

The transformation of rotating is $r = r'$, $\theta = \theta' + \theta_0$ for $0 < r' < r_1$, and $\theta = \theta' + h(r - r_2)$ for $r_1 < r' < r_2$. Here $h = \theta_0/(r_1 - r_2)$, and θ_0 is rotating angle. We can derive the Jacobian matrix in the core as $\tilde{J} = \text{diag}[1,\ 1]$, and that in the shell as $\tilde{J} = [(1,\ 0),\ (hr,\ 1)]$. The initial wave-like temperature profile in the core turns into $T = 40\sin\left[\beta(x\cos\theta_0 + y\sin\theta_0)\right] + 323$ K, and that in the shell turns into $T = 40\sin\{\beta\{x\cos[h(r-r_2)] + y\sin[h(r-r_2)]\}\} + 323$ K [see Fig. 3(d)]. The thermal waves at $t = 10$ s and $t = 20$ s are shown in Fig. 3(e) and (f), respectively. We can observe that the direction of thermal wave in the center is rotated by $\theta_0 = \pi/6$ anticlockwise.

Here we only apply a single transformation to realize a single function on one device. If one conducts transformation twice, it is possible to design devices with bifunctions of cloaking-rotating [18] and concentrating-rotating [19].

4. Experimental suggestions for transformation complex thermotics

Essentially, the transformation of τ [Eq. (11c)] is just the transformation of $\boldsymbol{v}$ [Eq. (13)], which is mathematically easy, but experimentally difficult. Meanwhile, we should transform the density and heat capacity of moving matter, which is also experimentally difficult. Fortunately, many fluid models can help [20–29]. Here we utilize a porous medium [20] to proceed. Then, we should extend transformation complex thermotics from pure materials to composite materials. The porous medium is composed of solid and fluid with solid porosity of ϕ. We denote the density and heat capacity of the solid (or fluid) as ρ_s (or ρ_f) and C_s (or C_f), respectively. The effective density (ρ) and heat capacity (C) of the porous medium can be derived from the weighted average of the solid and fluid, say, $\rho C = \phi\rho_f C_f + (1-\phi)\rho_s C_s$. Similar to Eq. (2), the complex thermal conductivities of the solid and fluid can be expressed as

$$\kappa_s = \sigma_s + \mathrm{i}\tau_s = \sigma_s + \mathrm{i}\frac{\rho_s C_s \boldsymbol{v}_s \cdot \boldsymbol{\beta}}{\beta^2}, \tag{14a}$$

$$\kappa_f = \sigma_f + \mathrm{i}\tau_f = \sigma_f + \mathrm{i}\frac{\rho_f C_f \boldsymbol{v}_f \cdot \boldsymbol{\beta}}{\beta^2}, \tag{14b}$$

where $\boldsymbol{v}_s$ and $\boldsymbol{v}_f$ are the velocities of the solid and fluid, respectively. The imaginary part of Eq. (14a) generally vanishes ($\tau_s = 0$) when the solid does not move ($\boldsymbol{v}_s = 0$). It is reasonable to handle the real parts of Eq. (14) with the method of weighted average, thus yielding the real part of the effective complex thermal conductivity as $\sigma = \phi\sigma_f + (1-\phi)\sigma_s$ [30]. The next question is how to treat the imaginary parts of Eq. (14). We know that the imaginary part τ of the effective complex thermal conductivity is related to propagation, which has vector property to some extent. Therefore, it is also physical to use the method of weighted average to derive the effective imaginary part, say, $\tau = \phi\tau_f + (1-\phi)\tau_s$. Therefore, the effective complex thermal conductivity κ of the porous medium can be expressed as

$$\kappa = \sigma + \mathrm{i}\tau = \phi\sigma_f + (1-\phi)\sigma_s + \mathrm{i}\left[\phi\tau_f + (1-\phi)\tau_s\right] \equiv \phi\kappa_f + (1-\phi)\kappa_s. \tag{15}$$

Eq. (15) is the second key result of this work, revealing the effective complex thermal conductivity of composite materials. By substituting Eq. (15) into Eq. (1), we obtain the dispersion relation in the porous medium,

$$\omega = \frac{\phi\rho_f C_f}{\rho C}\boldsymbol{v}_f \cdot \boldsymbol{\beta} + \frac{(1-\phi)\rho_s C_s}{\rho C}\boldsymbol{v}_s \cdot \boldsymbol{\beta} - \mathrm{i}\frac{\sigma\beta^2}{\rho C}. \tag{16}$$

When $\phi = 1$, the porous medium becomes pure fluid, and Eq. (16) is reduced to Eq. (3) naturally. Eq. (16) also echoes with the result obtained by directly solving the conduction-convection equation in a porous medium, and detailed derivations can be found in the Appendix.

With the understanding of Eq. (15), we can still use the result of Eq. (11), but it is not enough. We should consider the Darcy law and mass conservation. The Darcy law indicates that the origin of convective velocity is pressure difference, say, $\boldsymbol{v} = -(\eta/\xi)\nabla P$ where η is permeability, ξ is dynamic viscosity, and P denotes pressure. Since the pressure field is stable, density does not change with time and mass conservation is satisfied naturally. With these two physical conditions, we can obtain the transformation rule in a porous medium,

$$\left(\rho_f C_f\right)' = \rho_f C_f, \tag{17a}$$

$$\sigma_f' = \sigma_f, \tag{17b}$$

$$(\rho_s C_s)' = \left[(\rho C)' - \phi\rho_f C_f\right]/(1-\phi), \tag{17c}$$

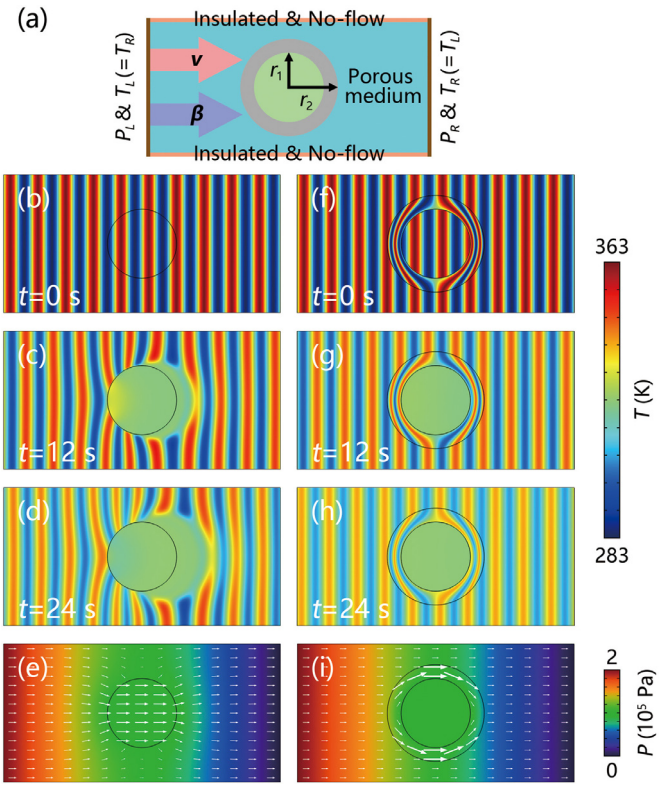

Fig. 4. (a) Schematic diagram of cloaking with a porous medium. (b)-(d) Temperature profiles and (e) pressure distribution with an obstacle located in the center. (f)-(h) Temperature profiles and (i) pressure distribution with the same obstacle coated by a cloak. White arrows in (e) and (i) denote convective velocities. $P_L = 2 \times 10^5$ Pa and $P_R = 0$ Pa. The fluid is still water with $\rho_f = 1000$ kg/m^3, $C_f = 4200$ J kg^{-1} K^{-1}, $\sigma_f = 0.6$ W m^{-1} K^{-1}, and $\xi = 10^{-3}$ Pa s. The background solid is stone with parameters $\rho_s = 4000$ kg/m^3, $C_s = 840$ J kg^{-1} K^{-1}, $\sigma_s = 2$ W m^{-1} K^{-1}, $\eta = 10^{-12}$ m^2, and $\phi = 0.8$. The obstacle has only different parameters of $\sigma = 400$ W m^{-1} K^{-1} and $\eta = 2 \times 10^{-10}$ m^2 from the background solid. The parameters in the shell are transformed as Eq. (17).

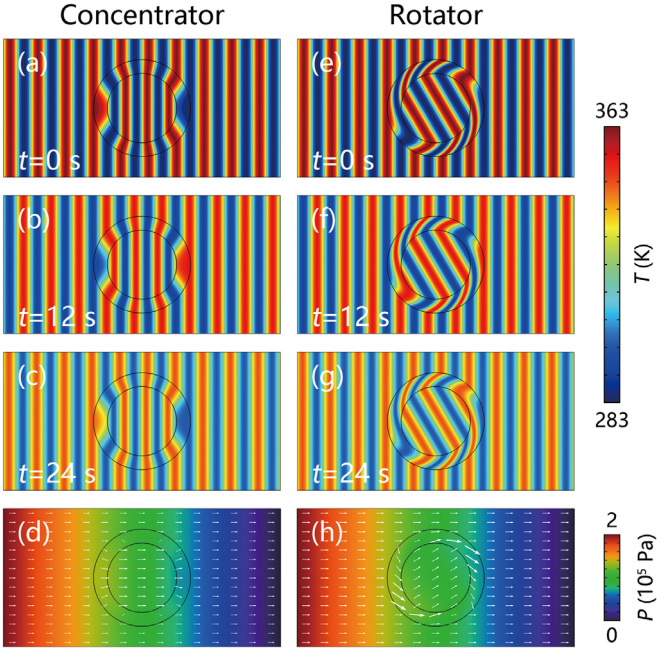

Fig. 5. Simulations of (a)-(d) concentrating and (e)-(g) rotating with a porous medium. The system sizes and background parameters are the same as those for Fig. 4. Other parameters are designed with Eq. (17).

$$\sigma'_s = \left(\sigma' - \phi\sigma_f\right)/(1-\phi), \tag{17d}$$

$$\eta' = \tilde{J}\eta\tilde{J}^S/\det\tilde{J}, \tag{17e}$$

where $(\rho C)'$ and σ' are determined by Eqs. (11a) and (11b), respectively. Eq. (17) is the third key result of this work, revealing the theory of transformation complex thermotics in a porous medium. Clearly, we only transform the parameters of solid, and avoid transforming convective velocity or moving fluid directly. Therefore, the physical problems for experiment have been solved, and the remaining problems are to seek for practical materials with anisotropic and inhomogeneous thermal conductivities and permeabilities, which have been widely studied such as multilayered structures [31–40]. Meanwhile, simultaneously applying a thermal field and a fluid field requires elaborate experimental apparatus.

Fig. 4 (a) shows the schematic diagram of our experimental suggestion. We use two modules including the heat transfer in a porous media and the Darcy law. The left and right boundaries are additionally set at high pressure (P_L) and low pressure (P_R), respectively. We take the wave vector $\beta = 2\pi m/W$ with $m = 10$, and the period of the thermal wave is $t_0 = 24$ s according to Eq. (16) with $\boldsymbol{v}_s = 0$. The initial wave-like temperature profiles [see Figs. 4(b) and 4(f)] are the same as those in Figs. 2(b) and 2(e). Clearly, if there does not exist a cloak coating the obstacle, the thermal wave [Figs. 4(c) and 4(d)] and the pressure field [Fig. 4(e)] are strongly distorted. In contrast, a cloak can avoid the distortion of the thermal wave [Figs. 4(g) and 4(h)] and the pressure field [Fig. 4(i)]. The thermal wave in Fig. 4(h) has also amplitude loss because of the positive real part of κ. After propagating for one period (24 s), the thermal wave in Fig. 4(h) approximately gains a phase difference of 2π, thus being at the same position as Fig. 4(f). We also provide experimental suggestions for concentrating and rotating whose parameters are designed according to Eq. (17). The simulation results are shown in Fig. 5(a)–(d) and Fig. 5(e)–(h), respectively. The concentrating and rotating effects are achieved indeed with a porous media. Therefore, the predictions of Eqs. (15)–(17) are physical, confirming the feasibility of transformation complex thermotics in composite materials. Certainly, the applications of transformation complex thermotics are not limited to the above three devices. Many other applications can also be expected such as camouflaging [41–52].

5. Conclusion

In summary, we have coined a complex thermal conductivity κ and the complex conduction equation (say, complex thermotics) to unify conduction and convection. The real and imaginary parts of κ correspond to conduction and convection, respectively. We have also proved the form-invariance of the complex conduction equation under coordinate transformations and derived the transformation principle of complex thermal conductivities. The theory of transformation complex thermotics allows us to control thermal waves flexibly. Three devices have been designed with functions of cloaking, concentrating, and rotating. Experimental suggestions are also provided with the method of weighted average to derive the effective complex thermal conductivity of composite materials such as porous media. These results extend the connotation of thermal conductivity from real number to complex number, which not only have fundamental relevance, but also have potential applications in controlling thermal waves based on metamaterials.

Declaration of Competing Interest

The authors declare that there are no conflicts of interest.

CRediT authorship contribution statement

Liujun Xu: Formal analysis, Writing - original draft. **Jiping Huang:** Formal analysis, Writing - original draft.

Acknowledgments

We acknowledge the financial support by the National Natural Science Foundation of China under Grant no. 11725521.

The conduction-convection equation in a porous medium is derived as follows. The conductive energy density $\boldsymbol{E}_1$ is

$$\boldsymbol{E}_1 = -\sigma\boldsymbol{\nabla}T. \tag{A1}$$

The convective energy density induced by the moving fluid $\boldsymbol{E}_2$ is

$$\boldsymbol{E}_2 = \phi\rho_f C_f \boldsymbol{v}_f T, \tag{A2}$$

and that induced by the moving solid $\boldsymbol{E}_3$ is

$$\boldsymbol{E}_3 = (1-\phi)\rho_s C_s \boldsymbol{v}_s T. \tag{A3}$$

Therefore, the total energy E that flows into the closed surface Σ from time t_1 to t_2 is

$$E = -\int_{t_1}^{t_2}\oiint_{\Sigma}\boldsymbol{n}\cdot(\boldsymbol{E}_1+\boldsymbol{E}_2+\boldsymbol{E}_3)d\boldsymbol{S}dt = -\int_{t_1}^{t_2}\iiint_{\Omega}\boldsymbol{\nabla}\cdot(\boldsymbol{E}_1+\boldsymbol{E}_2+\boldsymbol{E}_3)dVdt, \tag{A4}$$

where Ω is the region enclosed by the surface Σ, $\boldsymbol{n}$ is unit normal vector, dS is surface element, and dV is volume element.

On the other hand, the absorbed energy E' can be also derived from the thermodynamic formula

$$E' = \iiint_{\Omega}[\rho CT(t_2)-\rho CT(t_1)]dV = \int_{t_1}^{t_2}\iiint_{\Omega}\rho C(\partial T/\partial t)dVdt. \tag{A5}$$

According to the law of energy conservation, there must be $E = E'$, and we can derive the energy equation of the conduction-convection process in a porous medium as

$$\rho C\partial T/\partial t + \boldsymbol{\nabla}\cdot\left[-\sigma\boldsymbol{\nabla}T + \phi\rho_f C_f\boldsymbol{v}_f T + (1-\phi)\rho_s C_s\boldsymbol{v}_s T\right] = 0. \tag{A6}$$

With the definition of the effective complex thermal conductivity in a porous medium [say, Eq. (15) in the main text], Eq. (A6) can be reduced to

$$\rho C\partial T/\partial t + \boldsymbol{\nabla}\cdot(-\kappa\boldsymbol{\nabla}T) = 0. \tag{A7}$$

Therefore, the conduction-convection process in a porous medium is still dominated by the complex conduction equation where ρC and κ are the weighted average of the solid and fluid. We use the plane-wave solution [$T = A_0 e^{i(\boldsymbol{\beta}\cdot\boldsymbol{r}-\omega t)} + T_0$], and derive the dispersion relation as Eq. (16) in the main text. Consequently, Eqs. (15) and (16) in the main text are physically correct.

References

[1] S. Guenneau, D. Petiteau, M. Zerrad, C. Amra, T. Puvirajesinghe, Transformed fourier and fick equations for the control of heat and mass diffusion, AIP Adv. 5 (2015) 053404.
[2] G.L. Dai, J. Shang, J.P. Huang, Theory of transformation thermal convection for creeping flow in porous media: cloaking, concentrating, and camouflage, Phys. Rev. E 97 (2018) 022129.
[3] L.J. Xu, S. Yang, G.L. Dai, J.P. Huang, Transformation omnithermotics: simultaneous manipulation of three basic modes of heat transfer, ES Energy Environ. 7 (2020) 65–70.
[4] L.J. Xu, J.P. Huang, Negative thermal transport in conduction and advection, submitted.
[5] Y. Li, Y.-G. Peng, L. Han, M.-A. Miri, W. Li, M. Xiao, X.-F. Zhu, J.L. Zhao, A. Alú, S.H. Fan, C.W. Qiu, Anti-parity-time symmetry in diffusive systems, Science 364 (2019) 170–173.
[6] P.C. Cao, L. Y, Y.G. Peng, C.W. Qiu, X.F. Zhu, High-order exceptional points in diffusive systems: robust APT symmetry against perturbation and phase oscillation at APT symmetry breaking, ES Energy Environ. 7 (2020) 48–55.
[7] M. Farhat, P.-Y. Chen, H. Bagci, C. Amra, S. Guenneau, A. Alú, Thermal invisibility based on scattering cancellation and mantle cloaking, Sci. Rep. 5 (2015) 9876.
[8] M. Farhat, S. Guenneau, P.-Y. Chen, A. Alú, K.N. Salama, Scattering cancellation-based cloaking for the Maxwell-Cattaneo heat waves, Phys. Rev. Appl. 11 (2019) 044089.
[9] C.Z. Fan, Y. Gao, J.P. Huang, Shaped graded materials with an apparent negative thermal conductivity, Appl. Phys. Lett. 92 (2008) 251907.
[10] T.Y. Chen, C.-N. Weng, J.S. Chen, Cloak for curvilinearly anisotropic media in conduction, Appl. Phys. Lett. 93 (2008) 114103.
[11] Y.X. Liu, W.L. Guo, T.C. Han, Arbitrarily polygonal transient thermal cloaks with natural bulk materials in bilayer configurations, Int. J. Heat Mass Transf. 115 (2017) 1–5.
[12] J. Guo, Z.G. Qu, Thermal cloak with adaptive heat source to proactively manipulate temperature field in heat conduction process, Int. J. Heat Mass Transf. 127 (2018) 1212–1222.
[13] J. Qin, W. Luo, P. Yang, B. Wang, T. Deng, T.C. Han, Experimental demonstration of irregular thermal carpet cloaks with natural bulk material, Int. J. Heat Mass Transf. 141 (2019) 487–490.
[14] E. Dede, T. Nomura, J. Lee, Thermal-composite design optimization for heat flux shielding, focusing, and reversal, Struct. Multidiscip. Optim. 49 (2014) 59–68.
[15] G. Fujii, Y. Akimoto, M. Takahashi, Exploring optimal topology of thermal cloaks by CMA-ES, Appl. Phys. Lett. 112 (2018) 061108.
[16] G. Fujii, Y. Akimoto, Topology-optimized thermal carpet cloak expressed by an immersed-boundary level-set method via a covariance matrix adaptation evolution strategy, Int. J. Heat Mass Transf. 137 (2019) 1312–1322.
[17] G. Fujii, Y. Akimoto, Optimizing the structural topology of bifunctional invisible cloak manipulating heat flux and direct current, Appl. Phys. Lett. 115 (2019) 174101.
[18] L.L. Zhou, S.Y. Huang, M. Wang, R. Hu, X.B. Luo, While rotating while cloaking, Phys. Lett. A 383 (2019) 759–763.
[19] Y.-L. Tsai, J.Y. Li, T.Y. Chen, Simultaneous focusing and rotation of a bifunctional thermal metamaterial with constant anisotropic conductivity, J. Appl. Phys. 126 (2019) 095103.
[20] Y.A. Urzhumov, D.R. Smith, Fluid flow control with transformation media, Phys. Rev. Lett. 107 (2011) 074501.
[21] Y.A. Urzhumov, D.R. Smith, Flow stabilization with active hydrodynamic cloaks, Phys. Rev. E 86 (2012) 056313.
[22] P.T. Bowen, Y.A. Urzhumov, D.R. Smith, Wake control with permeable multilayer structures: the spherical symmetry case, Phys. Rev. E 92 (2015) 063030.
[23] J. Park, J.R. Youn, Y.S. Song, Hydrodynamic metamaterial cloak for drag-free flow, Phys. Rev. Lett. 123 (2019) 074502.
[24] J. Park, J.R. Youn, Y.S. Song, Fluid-flow rotator based on hydrodynamic metamaterial, Phys. Rev. Appl. 12 (2019) 061002.
[25] Z.Y. Wang, C.Y. Li, R. Zatianina, P. Zhang, Y.Q. Zhang, Carpet cloak for water waves, Phys. Rev. E 96 (2017) 053107.
[26] C.Y. Li, L. Xu, L.L. Zhu, S.Y. Zou, Q.H. Liu, Z.Y. Wang, H.Y. Chen, Concentrators for water waves, Phys. Rev. Lett. 121 (2018) 104501.
[27] S.Y. Zou, Y.D. Xu, R. Zatianina, C.Y. Li, X. Liang, L.L. Zhu, Y.Q. Zhang, G.H. Liu, Q.H. Liu, H.Y. Chen, Z.Y. Wang, Broadband waveguide cloak for water waves, Phys. Rev. Lett. 123 (2019) 074501.
[28] Y. Li, K.-J. Zhu, Y.-G. Peng, W. Li, T.Z. Yang, H.-X. Xu, H. Chen, X.-F. Zhu, S.H. Fan, C.W. Qiu, Thermal meta-device in analogue of zero-index photonics, Nat. Mater. 18 (2019) 48–54.
[29] L.J. Xu, J.P. Huang, Chameleonlike metashells in microfluidics: a passive approach to adaptive responses, Sci. China-Phys. Mech. Astron. 63 (2020) 228711.
[30] J. Bear, M.Y. Corapcioglu, Fundamentals of Transport Phenomena in Porous Media, Springer, Netherlands, 1984.
[31] K.P. Vemuri, P.R. Bandaru, Geometrical considerations in the control and manipulation of conductive heat flux in multilayered thermal metamaterials, Appl. Phys. Lett. 103 (2013) 133111.
[32] T.Z. Yang, K.P. Vemuri, P.R. Bandaru, Experimental evidence for the bending of heat flux in a thermal metamaterial, Appl. Phys. Lett. 105 (2014) 083908.
[33] K.P. Vemuri, F.M. Canbazoglu, P.R. Bandaru, Guiding conductive heat flux through thermal metamaterials, Appl. Phys. Lett. 105 (2014) 193904.
[34] J. Shang, R.Z. Wang, C. Xin, G.L. Dai, J.P. Huang, Macroscopic networks of thermal conduction: failure tolerance and switching processes, Int. J. Heat Mass Transf. 121 (2018) 321–328.
[35] L.J. Xu, S. Yang, J.P. Huang, Thermal theory for heterogeneously architected structure: fundamentals and application, Phys. Rev. E 98 (2018) 052128.
[36] L.J. Xu, S. Yang, J.P. Huang, Thermal transparency induced by periodic interparticle interaction, Phys. Rev. Appl. 11 (2019) 034056.
[37] J.X. Li, Y. Li, T.L. Li, W.Y. Wang, L.Q. Li, C.W. Qiu, Doublet thermal metadevice, Phys. Rev. Appl. 11 (2019) 044021.
[38] L.J. Xu, J.P. Huang, Metamaterials for manipulating thermal radiation: transparency, cloak, and expander, Phys. Rev. Appl. 12 (2019) 044048.
[39] G.L. Dai, J.P. Huang, Nonlinear thermal conductivity of periodic composites, Int. J. Heat Mass Transfer 147 (2020) 118917.
[40] J.P. Huang, Theoretical Thermotics: Transformation Thermotics and Extended Theories for Thermal Metamaterials, Springer, 2020.
[41] Y. Li, X. Bai, T.Z. Yang, H. Luo, C.W. Qiu, Structured thermal surface for radiative camouflage, Nat. Commun. 9 (2018) 273.
[42] R. Hu, S.L. Zhou, Y. Li, D.Y. Lei, X.B. Luo, C.W. Qiu, Illusion thermotics, Adv. Mater. 30 (2018) 1707237.
[43] R. Hu, S.Y. Huang, M. Wang, L.L. Zhou, X.Y. Peng, X.B. Luo, Binary thermal encoding by energy shielding and harvesting units, Phys. Rev. Appl. 10 (2018) 054032.
[44] S.L. Zhou, R. Hu, X.B. Luo, Thermal illusion with twinborn-like heat signatures, Int. J. Heat Mass Transf. 127 (2018) 607–613.
[45] R. Hu, S.Y. Huang, M. Wang, X.L. Luo, J. Shiomi, C.W. Qiu, Encrypted thermal printing with regionalization transformation, Adv. Mater. 31 (2019) 1807849.
[46] R. Hu, X.B. Luo, Two-dimensional phonon engineering triggers microscale thermal functionalities, Natl. Sci. Rev. 6 (2019) 1071–1073.
[47] L.J. Xu, S. Yang, J.P. Huang, Passive metashells with adaptive thermal conductivities: chameleonlike behavior and its origin, Phys. Rev. Appl. 11 (2019) 054071.
[48] X.Y. Peng, R. Hu, Three-dimensional illusion thermotics with separated thermal illusions, ES Energy Environ. 6 (2019) 39–44.
[49] F.B. Yang, L.J. Xu, J.P. Huang, Thermal illusion of porous media with convection-diffusion process: transparency, concentrating, and cloaking, ES Energy Environ. 6 (2019) 45–50.
[50] L.J. Xu, S. Yang, J.P. Huang, Dipole-assisted thermotics: experimental demonstration of dipole-driven thermal invisibility, Phys. Rev. E 100 (2019) 062108.
[51] R. Hu, S. Iwamoto, L. Feng, S.H. Ju, S.Q. Hu, M. Ohnishi, N. Nagai, K. Hirakawa, J. Shiomi, Machine-learning-optimized aperiodic superlattice minimizes coherent phonon heat conduction, Phys. Rew. X 10 (2020) 021050.
[52] Y.D. Liu, J.L. Song, W.X. Zhao, X.C. Ren, Q. Cheng, X.B. Luo, N.X.L. Fang, R. Hu, Dynamic thermal camouflage via a liquid-crystalbased radiative metasurface, Nanophotonics 9 (2020) 855–863.